MF only

NASA TECHNICAL TRANSLATION

NASA TT F- 14427

# STELLAR EVOLUTION, V
# THE CARBON-FLASH IN A STAR OF 5 SOLAR MASSES

R. Kippenhahn, H.-C. Thomas and A. Weigert



Translation of an article in Zeitschrift fuer Astrophysik (Journal of Astrophysics), Vol. 64, 1966, pp. 373-394.

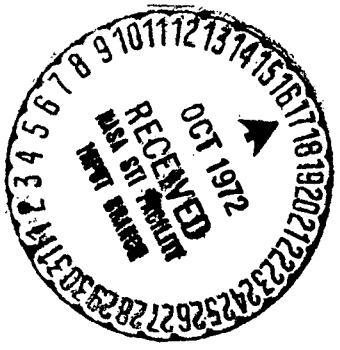


NATIONAL AERONAUTICS AND SPACE ADMINISTRATION
WASHINGTON, D. C. 20546 JUNE 1972

Wem 24

Source: Zeitschrift fuer
Astrophysik 64,373-394(1966)
The Max-Planck Institut fuer
Physik & Astrophysik, Munich

---

# Stellar Evolution. V

## The Carbon-Flash in a Star of 5 Solar Masses

R. Kippenhahn, H.-C. Thomas, and A. Weigert

Received, May 20, 1966

The onset of carbon burning in a star of 5 solar masses after exhaustion of its central helium content is computed. Since the ignition of carbon takes place in a degenerate region, the flash phenomenon occurs. The computations are carried out until degeneracy is removed and nuclear burning becomes stable. During this phase the helium burning shell becomes less and less important as the hydrogen is again ignited at the interface between the outer hydrogen-rich envelope and the helium core. No neutrino processes due to weak interaction (such as plasma neutrino or photo-neutrino emission) are taken into account.

## 1. Introduction

In the present paper the phase of fast carbon-burning of a star of the population I of 5 solar masses will be described. This phase follows immediately after the evolution which has been described in Part IV of this series (Kippenhahn, Thomas, Weigert, 1965). The publication is based on 171 consecutive stellar models which cover the period of 13 900 years before the carbon flash until 11 700 years thereafter.

The onset of nuclear burning shows considerably different characteristics depending upon the interior of the star and whether it is degenerate or not. In a star with non-degenerate interior, nuclear burning commences slowly and in a stable form (cf. appendix). If, however, nuclear burning starts in the degenerate core of a star, thermal instability is present: the central temperature and thus the energy production increase rapidly to values so high that $L_r$ in the central portion of the star amounts temporarily to a multiple of the outside luminosity. The thermal runaway lasts until the central temperature is so high that the degeneracy is abolished. The entire phenomenon is known as flash. It was first predicted by Mestel (1952) and

discovered by Schwarzschild and Härm (1962) at the onset of helium-burning in a star of 1.3 solar masses.

Depending upon the degree of degeneracy, all transitions from stable burning to the strong flash are encountered. At 1.3 $M_\odot$ degeneracy is large at the onset of helium burning ($\Psi \sim 20$), one observes a strong flash. At the onset of helium-burning in the interior of the 5 $M_\odot$-star described here degeneracy was quite weak ($\Psi \sim 0$); burning was, therefore, practically stable at the onset. At the time of contraction after the helium-burning, however, $\Psi$ had increased to approximately 9. It may thus be expected that the carbon-burning now begins with a moderate flash.

This case has the great advantage that the changes in the star are fast with regard to time and relative to other evolutionary phases; they are, however, slow with regard to the rate of attaining hydrostatic equilibrium. Inertia may, therefore, be neglected.

## 2. The Program

The computer program used is in essence the same as that used in Part IV of this series for the calculations described there. Several changes, however, turned out to

be a necessity.

The variable $\ln L_r$, used thus far, was replaced, beginning with Modell Nr. 451, by

$$\ln \left(1 + \frac{L_r}{L_0}\right) .$$

Here, $L_0 > 0$ is a suitably chosen constant. In the calculations $L_0$ was frequently assumed to be $\frac{1}{5} \cdot L$ ( L = outside luminosity of the model). With the new variable, $L_r$ may also become negative to almost $L_r = -L_0$. In our completed model negative luminosities were at no time observed, though the luminosity $L_r$ becomes very small outside of the carbon burning core (cf. section 3); during the iteration an approximation of $L_r$ may sometimes become negative. Furthermore, the singularity of the variables (which previously was at $L_r = 0$) is now further removed from the $L_r$ - values which occur in the calculation. With the introduction of this new variable, the system of the differential equation changes by which the differential equations are approximated. This results in a discontinuity in our calculations which is most clearly expressed in the central values of density and temperature (Fig. 3). The central temperature of the new system differs from that of the old system by approximately 4.5%.

Like in the preceding publication IV the formulae of publication I of this series (Hofmeister, Kippenhahn, Weigert (1964), section 3d) were applied to the hydrogen and helium-burning. For the helium-burning, now simplified in this way, only the $3\alpha$-reaction is taken into consideration and, accordingly, pure $C^{12}$ was assumed to be the final product of central helium-burning. For the subsequent carbon burning, one must, however, take into consideration that in reality a portion of the carbon is converted to $O^{16}$. In a rough approximation the first model of the evolutionary series described here was therefore artificially modified by reducing by 1/2 the carbon content $X_C$ of the core (which after the helium-burning has the value $X_C = 0.96$). The assumed chemical composition of the core was therefore $X_C = 0.48$; the weight proportion of heavy elements (with the exception of carbon and oxygen) was, as before, 4.4% by weight. For the $O^{16}$ -content ($X_O$) the remaining 48 weight percent were inserted. This artificial change of the chemical composition of the core has no disadvantageous consequences for the convergence of the Henyey-method, since this modification does not strongly modify the molecular weight nor the opacity. The calculations carried out subsequently by Hofmeister (1966) with detailed helium-burning, resulted in an endproduct $X_C = 0.44$, $X_O = 0.52$, $X_{Ne} = 0$ for a 5 $M_\odot$-star. The artificial change of the chemical composition

of the core is thus justified. The next reaction to be expected upon sufficient increase in temperature was therefore certainly the carbon burning $C^{12} + C^{12}$. The shield factor for weak shielding was calculated according to

$$\ln f = 6.77 \cdot 10^{-3} \frac{\varrho^{1/2}}{T_8^{3/2}} \left[5 - 3 X_C + \frac{1}{2}\left(\frac{\partial \ln \varrho}{\partial \psi}\right)_T\right]^{1/2},$$

($T_8 = 10^{-8} \cdot T$, $\Psi$ = degeneracy parameter). This formula is obtained according to Salpeter (1954), if in a simplification, one makes there the following assumption $X_O = X_C + X_{Mg} = \frac{1}{2}$ ; the derivation $(\partial \ln \varrho / \partial \Psi)$ is the term $f'/f = \partial \ln F_{1/2}(\Psi)/\partial \Psi$ of Salpeter. For the ρ- and T-region of interest a transition is actually present between weak and strong shielding which, however, for reasons of simplicity, was not taken into consideration. According to Reeves (1965) the following equation was applied

$$\varepsilon_C = X_C^2 \frac{\varrho}{T_8^{2/3}} f \cdot \exp\left[103.02 - 84.16\left(\frac{10}{T_8} + 0.07\right)^{1/3}\right].$$

The resulting change in carbon content was calculsted according to

$$\frac{\partial X_C^{-1}}{\partial t} = \frac{\varepsilon^*}{E_C}$$

with $E_C = 5 \cdot 10^{17}$ erg/g, and where $\varepsilon^* = \varepsilon_C / N_C^2$ was assumed to be

constant during each time step. (Actually the entire change in chemistry is of no significance in the phase described in the following due to the short duration and despite of the high $\epsilon_C$-values.)

Energy losses, as brought about by photoneutrinos, plasma-neutrinos etc., were not taken into consideration. In order to understand their influence it would seem to be required to first carry out exact calculations of the corresponding evolutionary phases without neutrino-effects.

## 3. Results

At the end of the phases described in IV the star migrated in the H-R-diagram to the upper right hand corner and reached a maximum of luminosity with model Nr. 397 and a minimum of the effective temperature ($\log L/L_o = 4.210$, $\log T_o = 3.511$).

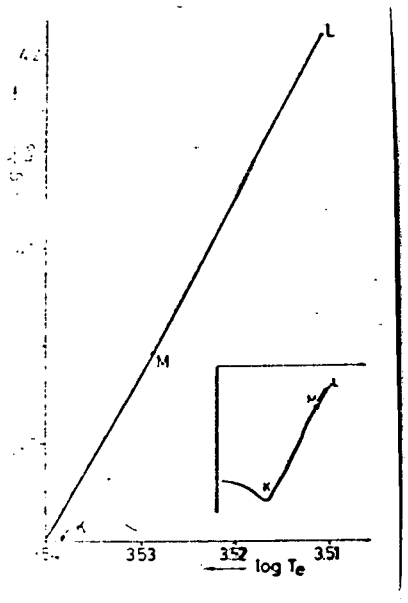


Figure 1. The evolutionary track in the H-R-diagram. Several significant points of the evolutionary track are indicated by capital letters (K,L,M). (The point not indicated between L and M represents the termination of the calculations). The exact coordinates and the corresponding age of the model can be found in Table 1. The insert to the lower right shows the relationship with the calculations published in Part IV of this series; the evolutionary sequence was spread between M and L in order to express clearly the direction of the evolution.

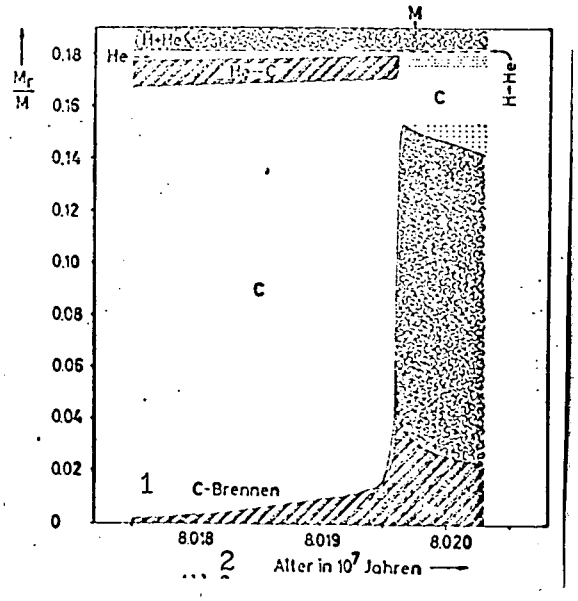


Figure 2. Changes in the interior of the star in dependence of time; $M_r/M$ is plotted versus the age of the star. "Cloudy" areas correspond to convective zones. Areas in which the nuclear energy production is larger than $10^3$ erg $g^{-1}$ $sec^{-1}$ are shaded. The hydrogen burning shell source (upper right) is so thin that it appears only as a dashed line. The areas in which the helium content Y and the carbon content $X_C$, respectively, decreased to the interior are dotted. Locations in which the carbon content is different from the initial chemistry by 0.01 or where the helium content is 0,01 were

1 carbon burning, 2 age in $10^7$ years

chosen as boundaries of the densest dotted areas. The same applies to the boundaries of the areas dotted at larger distances. The letter M refers to the corresponding location of the evolutionary process in Fig.1.

The evolutionary process in the H-R-diagram is simple during the phase discussed here, its course is evident from Fig.1. The evolutionary sequence comes from K and reaches L toward the end of the period of time discussed in IV. There it forms a spike, migrates then back within itself to M and returns and turns again in itself. The correlation between model Nr., age, and location in the H-R-diagram are given in Table 1.

Table 1. Coordinates in the H-R-diagram and age (in $10^7$ years) of several models

| 1 | 2 | | |
|---|---|---|---|
| Modell Nr. | Alter | $\log L/L_\odot$ | $\log T_e$ |
| 401 | 8.01822 | 4.207 | 3.511 |
| 402 | 8.01846 | 4.204 | 3.511 |
| 408 | 8.01942 | 4.161 | 3.516 |
| 419 | 8.01956 | 4.130 | 3.519 |
| 429 | 8.01959 | 4.121 | 3.520 |
| 439 | 8.01960 | 4.117 | 3.521 |
| 450 | 8.01961 | 4.115 | 3.521 |
| 461 | 8.01961 | 4.112 | 3.520 |
| 470 | 8.01961 | 4.111 | 3.520 |
| 480 | 8.01961 | 4.111 | 3.521 |
| 490 | 8.01961 | 4.109 | 3.521 |
| 494 | 8.01962 | 4.103 | 3.522 |
| 500 | 8.01964 | 4.048 | 3.529 |
| 501 | 8.01965 | 4.047 | 3.529 |
| 510 | 8.01988 | 4.123 | 3.519 |
| 520 | 8.02000 | 4.135 | 3.518 |
| 530 | 8.02015 | 4.139 | 3.518 |
| 540 | 8.02030 | 4.141 | 3.518 |
| 550 | 8.02045 | 4.141 | 3.518 |
| 560 | 8.02060 | 4.141 | 3.518 |
| 570 | 8.02075 | 4.141 | 3.518 |
| 572 | 8.02078 | 4.141 | 3.518 |

1 Model Nr.; 2 Age

The processes in the innermost 19% of the mass are plotted as function of time in Fig.2. The change of the central values of density and temperature is given in Fig.3. The change in luminosity $L_r/L$ in the central region is represented for several models in Fig.4. Fig.5 shows the behavior of $\frac{L_r}{L}$ in the shell sources of several models.

The central values of temperature and density of model 402 are $\log T_c = 8.651$ and $\log \rho_c = 6.718$, the degeneracy parameter is $\Psi = 9.2$. The radiative energy of the model originates to the extent of more than 95% from the helium-burning shell source at $\frac{M_r}{M} = 0.18$. The energy production by carbon-burning has just begun to be noticable; in the center is $\epsilon_C = 3 \cdot 10^3$ erg/g sec. Since here the contraction produces only $\epsilon_g = 5.7 \cdot 10^2$ erg/g sec[1)], the energy balance is practically solely determined by the carbon-burning at very high temperature exponents ($\sim 30$). The result is the run-up of the temperature at constant $\rho_c$ (cf. Fig.3) which is characteristic for the flash instability. For model 406, $\log T_c = 8.690$; the characteristic time for the temperature increase is here $\frac{dt}{d \ln T_c} = 2.2 \cdot 10^4$ a.

---

1) $\epsilon_g = -c_p \frac{\partial T}{\partial t} + \frac{\delta}{\rho} \frac{\partial P}{\partial t}$.

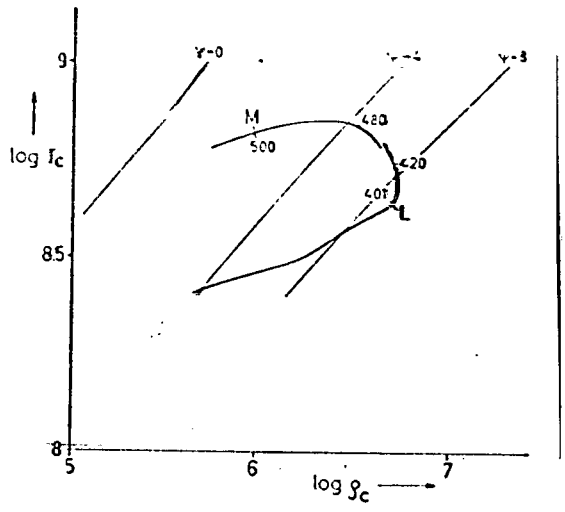


Figure 3. Central values of density and temperature during the evolution. The indicated model numbers refer to Table 1. The discontinuity of the curve between model 420 and 480 results from the intr duction of a new variable (cf. section 2). For a better understanding, several lines $\Psi$ = const. ($\Psi$ degeneracy parameter for hydrogen content X = 0) are inserted.

(For comparison: The time step chosen by the program for this model was $1.2 \cdot 10^3$ a. Thus the time step here and also in the following was always chosen in such a way that no significant changes of the model occur in it.) In the center of this model is $\rho_c = 5 \cdot 10^4$, $\epsilon_g = 1.4 \cdot 10^4$. The course of $L_r$ shows already a slight maximum in the vicinity of the center which increases further in the following models (cf. Fig.4). This is due to the fact that in the vicinity of the center $\frac{d L_r}{d M_r} = \epsilon_c + \epsilon_g > 0$, but becomes negative with increasing distance from the center, because $\epsilon_c$ ($> 0$) decreases strongly with the temperature while $\epsilon_g$ ($< 0$) varies by far not as much. Since the heat conductivity of the degenerate electron gas is large, it carried initially practically the entire energy transport. Accordingly, the effective $\varkappa$ is only approximately $2 \cdot 10^{-3}$. Despite of that, a considerable temperature gradient develops soon in the center since the flux of radiation increases here more and more. The maximum of luminosity increases with time and a convective core is therefore formed for Model 406 which in its mass grows more and more to the outside. Immediately outside of the convective core $L_o/L$ is always very small, namely lower than 0.01 (cf. Fig.4).

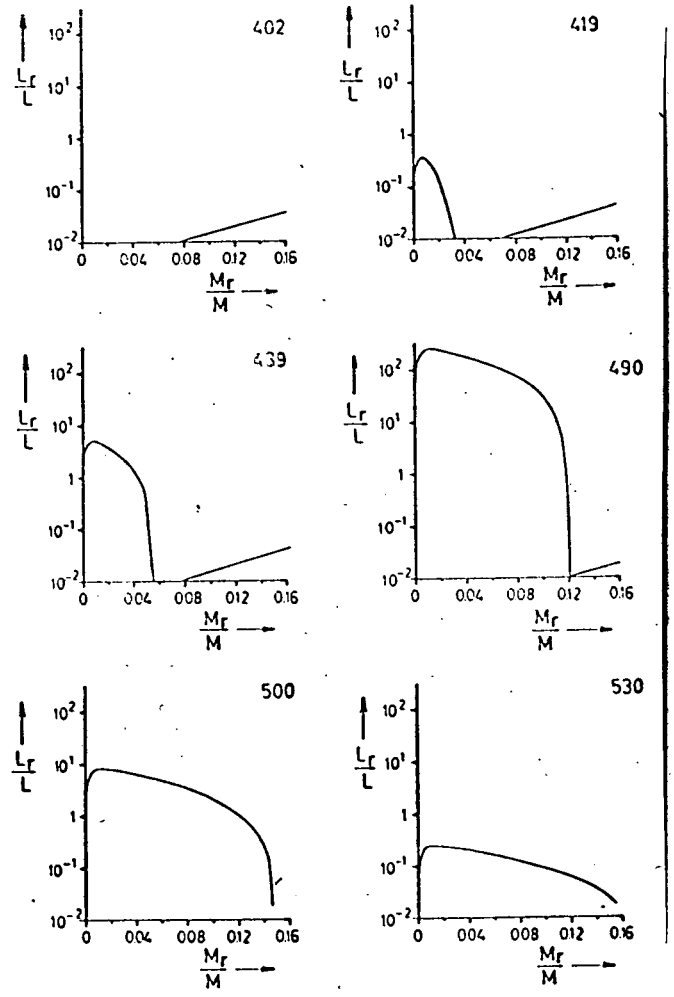


Figure 4. The luminosity $L_r/L$ in the central region of the star as function of $M_r/M$ for several models. The figures given indicate the model numbers.

The subsequent development of the central region with time has been compiled in Table 2. Since the evolution as a whole is relatively short the age of the model has not been given but rather the difference in age as apposed to model 401.

Table 2. Characteristic values in the center for several selected models. In the second column the age is given relative to Model 401. The last three columns contain the value of the luminosity maximum, its location, as well as the size of the convective core.

1 2

| Nr. | Alter in Jahren | Zentrum | | | | | | $L_{max}$ | | $\frac{M_K}{M}$ |
|---|---|---|---|---|---|---|---|---|---|---|
| | | $\log T$ | $\log \varrho$ | $\psi$ | $\varepsilon_C$ | $\varepsilon_\varrho$ | $(TT\dot{T})_H$ | $L_r/L$ | $M_r/M$ | |
| 402 | 2407.00 | 8.6513 | 6.718 | 9.2 | $2.44 \cdot 10^3$ | $-5.72 \cdot 10^3$ | $7.9 \cdot 10^6$ | — | — | — |
| 408 | 12034.20 | 8.7054 | 6.727 | 8.2 | $8.01 \cdot 10^4$ | $-2.12 \cdot 10^4$ | $8.1 \cdot 10^4$ | 0.02 | 0.004 | 0.010 |
| 419 | 13463.00 | 8.7427 | 6.714 | 7.3 | $9.64 \cdot 10^5$ | $-1.10 \cdot 10^5$ | $2.2 \cdot 10^4$ | 0.36 | 0.007 | 0.028 |
| 439 | 13857.80 | 8.7820 | 6.680 | 6.4 | $1.17 \cdot 10^7$ | $-7.89 \cdot 10^5$ | $3.0 \cdot 10^3$ | 5.06 | 0.009 | 0.053 |
| 461 | 13935.35 | 8.8016 | 6.624 | 5.6 | $3.08 \cdot 10^7$ | $-2.17 \cdot 10^6$ | $2.1 \cdot 10^3$ | 18.5 | 0.009 | 0.071 |
| 470 | 13961.20 | 8.8218 | 6.582 | 5.1 | $9.85 \cdot 10^7$ | $-6.19 \cdot 10^6$ | $9.4 \cdot 10^2$ | 61.6 | 0.009 | 0.084 |
| 480 | 13975.34 | 8.8394 | 6.517 | 4.4 | $2.43 \cdot 10^8$ | $-1.38 \cdot 10^7$ | $4.1 \cdot 10^2$ | 158. | 0.012 | 0.100 |
| 490 | 13988.31 | 8.8530 | 6.393 | 3.5 | $3.78 \cdot 10^8$ | $-1.93 \cdot 10^7$ | $1.7 \cdot 10^3$ | 253. | 0.012 | 0.119 |
| 494 | 14023.56 | 8.8465 | 6.197 | 2.6 | $1.24 \cdot 10^8$ | $-5.91 \cdot 10^6$ | $-4.0 \cdot 10^3$ | 86.5 | 0.012 | 0.136 |
| 500 | 14286.76 | 8.8201 | 5.989 | 1.9 | $1.05 \cdot 10^7$ | $-4.69 \cdot 10^5$ | $-1.7 \cdot 10^4$ | 8.34 | 0.012 | 0.148 |
| 510 | 16617.96 | 8.7918 | 5.821 | 1.4 | $8.67 \cdot 10^5$ | $-3.57 \cdot 10^4$ | $-1.9 \cdot 10^5$ | 0.57 | 0.012 | 0.148 |
| 530 | 10325.16 | 8.7826 | 5.772 | 1.3 | $3.90 \cdot 10^5$ | $-1.51 \cdot 10^4$ | $-4.3 \cdot 10^5$ | 0.25 | 0.012 | 0.144 |

1 Age in Years; 2 Center

The nuclear energy production increases with the central temperature and thus the maximum of luminosity (which in the course of time relocates its mass only insignificantly to the outside) and the mass $M_K$ of the convective core. A characteristic model for the initial phase of the flash is Nr. 419 which is presented in Table 3.

The maximum of temperature and the highest value of the luminosity maximum ($L_r = 253\ L = 3.9 \cdot 10^6\ L_\odot$) have been reached with Model 490. The fastest phase of the evolution had already been reached with Model 480. There the characteristic time for the increase in central temperature was at 400 years (the time step chosen by the program was 1.2 years). Thus, the evolution is there also so slow that, in very good approximation, the hydrostatic equilibrium is maintained at all times and that, in good approximation, the convection may be adjusted accordingly. The slowdown in evolution after Model 480, while the temperature is still rising, is due to the now significant expansion: Despite the fact, that with increasing luminosity the value of $\epsilon_g$ in the convective core increases further, i.e. per second more and more energy is still converted into inner energy and into work of expansion, this happens now to a lesser extent in favor of the inner energy. Since the degeneracy decreases, the work of expansion

Table 3. The Model Nr. 419

In the convective regions log T has been printed in italics

| $M_r/M$ | log $P$ | log $T$ | log $r$ | $L_r/L$ | log $\varrho$ | $X$ | $Y$ | $X_c$ |
|---|---|---|---|---|---|---|---|---|
| 0.9710 | 4.739 | *4.230* | 13.342 | 1.000 | —7.574 | 0.572 | 0.384 | 0.000 |
| 0.9145 | 5.081 | *4.365* | 13.314 | 1.000 | —7.368 | 0.572 | 0.384 | 0.000 |
| 0.8890 | 5.483 | *4.522* | 13.270 | 1.000 | —7.125 | 0.572 | 0.384 | 0.000 |
| 0.8019 | 5.862 | *4.668* | 13.213 | 1.000 | —6.895 | 0.572 | 0.384 | 0.000 |
| 0.6941 | 6.188 | *4.791* | 13.147 | 0.999 | —6.696 | 0.572 | 0.384 | 0.000 |
| 0.5832 | 6.460 | *4.892* | 13.075 | 0.999 | —6.529 | 0.572 | 0.384 | 0.000 |
| 0.4452 | 6.775 | *5.007* | 12.965 | 0.998 | —6.334 | 0.572 | 0.384 | 0.000 |
| 0.3631 | 6.981 | *5.080* | 12.875 | 0.998 | —6.205 | 0.572 | 0.384 | 0.000 |
| 0.2929 | 7.204 | *5.157* | 12.760 | 0.997 | —6.065 | 0.572 | 0.384 | 0.000 |
| 0.2333 | 7.519 | *5.264* | 12.578 | 0.996 | —5.866 | 0.572 | 0.384 | 0.000 |
| 0.2013 | 7.941 | *5.401* | 12.333 | 0.996 | —5.596 | 0.572 | 0.384 | 0.000 |
| 0.1890 | 8.485 | *5.571* | 12.052 | 0.996 | —5.243 | 0.572 | 0.384 | 0.000 |
| 0.1856 | 8.940 | *5.707* | 11.844 | 0.996 | —4.943 | 0.572 | 0.384 | 0.000 |
| 0.1835 | 9.614 | *5.902* | 11.568 | 0.995 | —4.495 | 0.572 | 0.384 | 0.000 |
| 0.1828 | 10.149 | *6.053* | 11.365 | 0.995 | —4.135 | 0.572 | 0.384 | 0.000 |
| 0.1824 | 10.703 | *6.205* | 11.166 | 0.995 | —3.759 | 0.572 | 0.384 | 0.000 |
| 0.1822 | 11.150 | *6.326* | 11.012 | 0.995 | —3.454 | 0.572 | 0.384 | 0.000 |
| 0.1820 | 11.752 | *6.488* | 10.809 | 0.995 | —3.040 | 0.572 | 0.384 | 0.000 |
| 0.1819 | 12.277 | 6.625 | 10.638 | 0.995 | —2.668 | 0.572 | 0.384 | 0.000 |
| 0.1818 | 12.928 | 6.781 | 10.444 | 0.995 | —2.154 | 0.572 | 0.384 | 0.000 |
| 0.1818 | 13.370 | 6.887 | 10.324 | 0.994 | —1.808 | 0.572 | 0.384 | 0.000 |
| 0.1817 | 13.841 | 7.004 | 10.202 | 0.994 | —1.451 | 0.572 | 0.384 | 0.000 |
| 0.1817 | 14.328 | 7.122 | 10.078 | 0.994 | —1.072 | 0.572 | 0.384 | 0.000 |
| 0.1816 | 14.815 | 7.242 | 9.957 | 0.993 | —0.702 | 0.572 | 0.384 | 0.000 |
| 0.1816 | 15.297 | 7.359 | 9.839 | 0.992 | —0.331 | 0.572 | 0.384 | 0.000 |
| 0.1815 | 15.706 | 7.458 | 9.740 | 0.991 | —0.011 | 0.572 | 0.384 | 0.000 |
| 0.1815 | 16.044 | 7.541 | 9.662 | 0.991 | 0.446 | 0.143 | 0.813 | 0.000 |
| 0.1814 | 16.430 | 7.620 | 9.615 | 0.990 | 0.876 | 0.000 | 0.956 | 0.000 |
| 0.1813 | 16.858 | 7.721 | 9.560 | 0.990 | 1.212 | 0.000 | 0.956 | 0.000 |
| 0.1811 | 17.375 | 7.848 | 9.487 | 0.988 | 1.605 | 0.000 | 0.956 | 0.000 |
| 0.1808 | 17.794 | 7.948 | 9.421 | 0.984 | 1.932 | 0.000 | 0.956 | 0.000 |
| 0.1804 | 18.259 | 8.058 | 9.345 | 0.978 | 2.295 | 0.000 | 0.956 | 0.000 |
| 0.1800 | 18.605 | 8.145 | 9.284 | 0.972 | 2.553 | 0.000 | 0.956 | 0.000 |
| 0.1792 | 19.131 | 8.277 | 9.184 | 0.926 | 2.952 | 0.000 | 0.916 | 0.040 |
| 0.1790 | 19.242 | 8.302 | 9.163 | 0.805 | 3.055 | 0.000 | 0.784 | 0.172 |
| 0.1789 | 19.295 | 8.312 | 9.153 | 0.700 | 3.114 | 0.000 | 0.663 | 0.293 |
| 0.1788 | 19.347 | 8.320 | 9.144 | 0.584 | 3.176 | 0.000 | 0.540 | 0.416 |
| 0.1787 | 19.396 | 8.326 | 9.136 | 0.480 | 3.238 | 0.000 | 0.422 | 0.534 |
| 0.1786 | 19.444 | 8.331 | 9.128 | 0.396 | 3.298 | 0.000 | 0.330 | 0.626 |
| 0.1784 | 19.512 | 8.338 | 9.117 | 0.306 | 3.380 | 0.000 | 0.231 | 0.725 |
| 0.1782 | 19.616 | 8.345 | 9.102 | 0.219 | 3.502 | 0.000 | 0.137 | 0.819 |
| 0.1774 | 19.859 | 8.360 | 9.070 | 0.130 | 3.764 | 0.000 | 0.045 | 0.911 |
| 0.1748 | 20.395 | 8.394 | 9.008 | 0.075 | 4.286 | 0.000 | 0.005 | 0.951 |
| 0.1697 | 20.924 | 8.446 | 8.947 | 0.056 | 4.750 | 0.000 | 0.001 | 0.955 |
| 0.1617 | 21.369 | 8.504 | 8.892 | 0.046 | 5.110 | 0.000 | 0.000 | 0.956 |
| 0.1484 | 21.802 | 8.545 | 8.831 | 0.035 | 5.455 | 0.000 | 0.000 | 0.956 |
| 0.1221 | 22.302 | 8.578 | 8.744 | 0.023 | 5.835 | 0.000 | 0.000 | 0.956 |
| 0.0930 | 22.662 | 8.599 | 8.660 | 0.015 | 6.096 | 0.000 | 0.000 | 0.956 |

Table 3.(contd.)

| $M_r/M$ | $\log P$ | $\log T$ | $\log r$ | $L_r/L$ | $\log \varrho$ | $X$ | $Y$ | $X_c$ |
|---|---|---|---|---|---|---|---|---|
| 0.0723 | 22.865 | 8.6[illegible] | 8.598 | 0.011 | 6.240 | 0.000 | 0.000 | 0.956 |
| 0.0584 | 22.987 | 8.6[illegible] | 8.551 | 0.009 | 6.327 | 0.000 | 0.000 | 0.956 |
| 0.0476 | 23.078 | 8.6[illegible] | 8.510 | 0.007 | 6.390 | 0.000 | 0.000 | 0.956 |
| 0.0357 | 23.177 | 8.6[illegible] | 8.454 | 0.007 | 6.455 | 0.000 | 0.000 | 0.956 |
| 0.0302 | 23.222 | 8.6[illegible] | 8.424 | 0.015 | 6.491 | 0.000 | 0.000 | 0.956 |
| 0.0280 | 23.240 | 8.6[illegible] | 8.411 | 0.030 | 6.503 | 0.000 | 0.000 | 0.953 |
| 0.0265 | 23.253 | 8.6[illegible] | 8.401 | 0.051 | 6.512 | 0.000 | 0.000 | 0.953 |
| 0.0246 | 23.268 | 8.6[illegible] | 8.388 | 0.083 | 6.522 | 0.000 | 0.000 | 0.953 |
| 0.0204 | 23.304 | 8.6[illegible] | 8.356 | 0.154 | 6.546 | 0.000 | 0.000 | 0.953 |
| 0.0156 | 23.347 | 8.6[illegible] | 8.311 | 0.237 | 6.575 | 0.000 | 0.000 | 0.953 |
| 0.0025 | 23.508 | 8.7[illegible] | 7.989 | 0.292 | 6.682 | 0.000 | 0.000 | 0.953 |
| 0.0023 | 23.512 | 8.7[illegible] | 7.973 | 0.278 | 6.685 | 0.000 | 0.000 | 0.953 |
| 0.0021 | 23.516 | 8.7[illegible] | 7.955 | 0.261 | 6.688 | 0.000 | 0.000 | 0.953 |
| 0.0000 | 23.554 | 8.7[illegible] | 1.000 | 0.000 | 6.714 | 0.000 | 0.000 | 0.953 |

Table 4. The Model Nr. 490

In the convective regions log T has been printed in italics

| $M_r/M$ | log $P$ | log $T$ | log $r$ | $L_r/L$ | log $\varrho$ | $X$ | $Y$ | $X_c$ |
|---|---|---|---|---|---|---|---|---|
| 0.9710 | 4.801 | *4.255* | 13.326 | 1.000 | —7.528 | 0.572 | 0.384 | 0.0000 |
| 0.9053 | 5.451 | *4.550* | 13.266 | 1.000 | —7.135 | 0.572 | 0.384 | 0.0000 |
| 0.7799 | 6.001 | *4.772* | 13.183 | 0.998 | —6.801 | 0.572 | 0.384 | 0.0000 |
| 0.6686 | 6.318 | *4.882* | 13.115 | 0.996 | —6.607 | 0.572 | 0.384 | 0.0000 |
| 0.5450 | 6.611 | *4.990* | 13.032 | 0.994 | —6.427 | 0.572 | 0.384 | 0.0000 |
| 0.4127 | 6.917 | *5.080* | 12.917 | 0.990 | —6.237 | 0.572 | 0.384 | 0.0000 |
| 0.2784 | 7.327 | *5.198* | 12.712 | 0.985 | —5.980 | 0.572 | 0.384 | 0.0000 |
| 0.2013 | 8.011 | *5.429* | 12.315 | 0.981 | —5.544 | 0.572 | 0.384 | 0.0000 |
| 0.1872 | 8.756 | *5.659* | 11.940 | 0.980 | —5.059 | 0.572 | 0.384 | 0.0000 |
| 0.1839 | 9.524 | *5.878* | 11.613 | 0.980 | —4.550 | 0.572 | 0.384 | 0.0000 |
| 0.1829 | 10.206 | *6.065* | 11.352 | 0.979 | —4.091 | 0.572 | 0.384 | 0.0000 |
| 0.1824 | 10.951 | *6.271* | 11.086 | 0.979 | —3.585 | 0.572 | 0.384 | 0.0000 |
| 0.1821 | 11.676 | *6.466* | 10.840 | 0.979 | —3.088 | 0.572 | 0.384 | 0.0000 |
| 0.1820 | 12.437 | 6.660 | 10.596 | 0.978 | —2.529 | 0.572 | 0.384 | 0.0000 |
| 0.1819 | 13.171 | 6.852 | 10.390 | 0.973 | —1.940 | 0.572 | 0.384 | 0.0000 |
| 0.1818 | 13.995 | 7.064 | 10.178 | 0.968 | —1.309 | 0.572 | 0.384 | 0.0000 |
| 0.1817 | 14.828 | 7.267 | 9.972 | 0.961 | —0.668 | 0.572 | 0.384 | 0.0000 |
| 0.1816 | 15.622 | 7.458 | 9.781 | 0.950 | —0.050 | 0.572 | 0.384 | 0.0000 |
| 0.1815 | 16.308 | 7.639 | 9.620 | 0.936 | 0.667 | 0.143 | 0.813 | 0.0000 |
| 0.1814 | 16.841 | 7.771 | 9.554 | 0.929 | 1.214 | 0.000 | 0.956 | 0.0000 |
| 0.1811 | 17.485 | 7.895 | 9.467 | 0.914 | 1.715 | 0.000 | 0.956 | 0.0000 |

Table 4. (contd.)

| $M_r/M$ | $\log P$ | $\log T$ | $\log r$ | $L_r/L$ | $\log \varrho$ | $X$ | $Y$ | $X_c$ |
|---|---|---|---|---|---|---|---|---|
| 0.1805 | 18.212 | 8.035 | 9.357 | 0.889 | 2.285 | 0.000 | 0.956 | 0.0000 |
| 0.1796 | 18.884 | 8.197 | 9.242 | 0.753 | 2.800 | 0.000 | 0.951 | 0.0025 |
| 0.1791 | 19.129 | 8.248 | 9.199 | 0.554 | 3.018 | 0.000 | 0.814 | 0.1418 |
| 0.1790 | 19.190 | 8.259 | 9.189 | 0.478 | 3.087 | 0.000 | 0.683 | 0.2734 |
| 0.1789 | 19.237 | 8.265 | 9.181 | 0.417 | 3.145 | 0.000 | 0.556 | 0.3995 |
| 0.1788 | 19.282 | 8.271 | 9.174 | 0.362 | 3.202 | 0.000 | 0.441 | 0.5151 |
| 0.1787 | 19.325 | 8.275 | 9.168 | 0.314 | 3.255 | 0.000 | 0.344 | 0.6115 |
| 0.1785 | 19.387 | 8.281 | 9.159 | 0.254 | 3.329 | 0.000 | 0.242 | 0.7141 |
| 0.1782 | 19.500 | 8.290 | 9.144 | 0.172 | 3.457 | 0.000 | 0.130 | 0.8260 |
| 0.1757 | 20.088 | 8.320 | 9.075 | 0.055 | 4.056 | 0.000 | 0.008 | 0.9476 |
| 0.1686 | 20.788 | 8.376 | 8.998 | 0.039 | 4.681 | 0.000 | 0.000 | 0.9556 |
| 0.1553 | 21.359 | 8.438 | 8.928 | 0.020 | 5.145 | 0.000 | 0.000 | 0.9560 |
| 0.1468 | 21.580 | 8.454 | 8.896 | 0.020 | 5.320 | 0.000 | 0.000 | 0.9560 |
| 0.1405 | 21.713 | 8.461 | 8.876 | 0.015 | 5.424 | 0.000 | 0.000 | 0.9560 |
| 0.1347 | 21.819 | 8.466 | 8.859 | 0.013 | 5.505 | 0.000 | 0.000 | 0.9560 |
| 0.1304 | 21.888 | 8.469 | 8.847 | 0.008 | 5.558 | 0.000 | 0.000 | 0.9560 |
| 0.1264 | 21.950 | 8.471 | 8.836 | 0.014 | 5.604 | 0.000 | 0.000 | 0.9560 |
| 0.1228 | 22.001 | 8.474 | 8.827 | 0.014 | 5.642 | 0.000 | 0.000 | 0.9560 |
| 0.1191 | 22.049 | 8.476 | 8.818 | 0.015 | 5.678 | 0.000 | 0.000 | 0.9560 |
| 0.1164 | 22.084 | *8.485* | 8.811 | 1.042 | 5.701 | 0.000 | 0.000 | 0.9419 |
| 0.1155 | 22.095 | *8.489* | 8.808 | 2.252 | 5.708 | 0.000 | 0.000 | 0.9419 |
| 0.1137 | 22.117 | *8.497* | 8.804 | 5.360 | 5.722 | 0.000 | 0.000 | 0.9419 |
| 0.1112 | 22.147 | *8.508* | 8.798 | 9.738 | 5.741 | 0.000 | 0.000 | 0.9419 |
| 0.1073 | 22.191 | *8.524* | 8.788 | 16.7 | 5.769 | 0.000 | 0.000 | 0.9419 |
| 0.0982 | 22.287 | *8.558* | 8.764 | 34.2 | 5.830 | 0.000 | 0.000 | 0.9419 |
| 0.0860 | 22.405 | *8.599* | 8.732 | 59.9 | 5.906 | 0.000 | 0.000 | 0.9419 |
| 0.0716 | 22.529 | *8.643* | 8.691 | 93.1 | 5.986 | 0.000 | 0.000 | 0.9419 |
| 0.0424 | 22.757 | *8.722* | 8.588 | 171. | 6.134 | 0.000 | 0.000 | 0.9419 |
| 0.0124 | 22.996 | *8.802* | 8.379 | 253. | 6.291 | 0.000 | 0.000 | 0.9419 |
| 0.0029 | 23.095 | *8.835* | 8.149 | 175. | 6.357 | 0.000 | 0.000 | 0.9419 |
| 0.0023 | 23.103 | *8.838* | 8.113 | 155. | 6.362 | 0.000 | 0.000 | 0.9419 |
| 0.0021 | 23.106 | *8.839* | 8.099 | 147. | 6.364 | 0.000 | 0.000 | 0.9419 |
| 0.0000 | 23.150 | *8.853* | | 0.000 | 6.393 | 0.000 | 0.000 | 0.9419 |

takes over a steadily increasing proportion and $\partial \ln T_c / \partial t$ becomes thus smaller.

Model 490 is represented in Table 4. Despite the fact that $L_r$ and $T_c$ assume their greatest values in this model, only to decrease subsequently, the convective core is still growing in mass. $M_K$ reaches a maximum of 0.154 M with Model 502. From now on the evolution becomes slower and slower, the maximum of $L_r$ in the convective core decreases rapidly, the central region expands and decreases simultaneously the temperature. Degeneracy has been removed to such an extent that stable nuclear burning may commence. The carbon originally present in the center is still practically completely available for this stable burning because, up to Model 541, only approximately 2% of the carbon have been burned during the short flash phase, despite the high $L_r$-values in the interior. The maximum luminosity in the interior was $L_r > 10$ L for approximately 300 years and > 100 L for 54 years.

In Table 5 the last of the calculated models (Nr. 572) is represented.

Table 5. The Model Nr. 572

In the convective regions log T has been printed in italics

| $M, M$ | log $P$ | log $T$ | log $r$ | $L_r/L$ | log $\varrho$ | $X$ | $Y$ | $X_c$ |
|---|---|---|---|---|---|---|---|---|
| 0.9710 | 4.707 | *4.222* | 13.350 | 1.000 | —7.599 | 0.572 | 0.384 | 0.000 |
| 0.9445 | 5.048 | *4.352* | 13.322 | 1.000 | —7.393 | 0.572 | 0.384 | 0.000 |
| 0.8890 | 5.450 | *4.511* | 13.278 | 1.000 | —7.151 | 0.572 | 0.384 | 0.000 |
| 0.8019 | 5.828 | *4.691* | 13.221 | 1.000 | —6.921 | 0.572 | 0.384 | 0.000 |
| 0.7188 | 6.087 | *4.754* | 13.170 | 1.000 | —6.763 | 0.572 | 0.384 | 0.000 |
| 0.6139 | 6.354 | *4.851* | 13.104 | 1.000 | —6.599 | 0.572 | 0.384 | 0.000 |
| 0.5450 | 6.514 | *4.916* | 13.056 | 1.000 | —6.500 | 0.572 | 0.384 | 0.000 |
| 0.4807 | 6.660 | *4.968* | 13.005 | 1.000 | —6.410 | 0.572 | 0.384 | 0.000 |
| 0.4127 | 6.820 | *5.022* | 12.941 | 1.000 | —6.310 | 0.572 | 0.384 | 0.000 |
| 0.3457 | 6.998 | *5.088* | 12.858 | 1.000 | —6.199 | 0.572 | 0.384 | 0.000 |
| 0.2784 | 7.232 | *5.176* | 12.734 | 1.000 | —6.052 | 0.572 | 0.384 | 0.000 |
| 0.2179 | 7.642 | *5.305* | 12.494 | 1.000 | —5.792 | 0.572 | 0.384 | 0.000 |
| 0.1950 | 8.131 | *5.462* | 12.222 | 1.000 | —5.477 | 0.572 | 0.384 | 0.000 |
| 0.1881 | 8.614 | *5.612* | 11.985 | 1.000 | —5.162 | 0.572 | 0.384 | 0.000 |
| 0.1852 | 9.175 | *5.779* | 11.740 | 1.000 | —4.791 | 0.572 | 0.384 | 0.000 |
| 0.1839 | 9.721 | *5.932* | 11.523 | 1.000 | —4.426 | 0.572 | 0.384 | 0.000 |
| 0.1833 | 10.256 | *6.087* | 11.323 | 1.000 | —4.065 | 0.572 | 0.384 | 0.000 |
| 0.1830 | 10.807 | *6.238* | 11.128 | 1.000 | —3.690 | 0.572 | 0.384 | 0.000 |
| 0.1828 | 11.319 | *6.377* | 10.953 | 1.000 | —3.340 | 0.572 | 0.384 | 0.000 |
| 0.1826 | 11.916 | *6.532* | 10.754 | 1.000 | —2.929 | 0.572 | 0.384 | 0.000 |
| 0.1825 | 12.527 | *6.688* | 10.559 | 1.000 | —2.484 | 0.572 | 0.384 | 0.000 |
| 0.1824 | 13.042 | 6.819 | 10.409 | 1.000 | —2.069 | 0.572 | 0.384 | 0.000 |
| 0.1824 | 13.509 | 6.926 | 10.284 | 1.000 | —1.711 | 0.572 | 0.384 | 0.000 |
| 0.1823 | 14.006 | 7.043 | 10.155 | 0.999 | —1.331 | 0.572 | 0.384 | 0.000 |
| 0.1823 | 14.518 | 7.173 | 10.026 | 0.999 | —0.935 | 0.572 | 0.384 | 0.000 |
| 0.1822 | 15.029 | 7.292 | 9.899 | 0.999 | —0.547 | 0.572 | 0.384 | 0.000 |
| 0.1822 | 15.531 | 7.414 | 9.776 | 0.998 | —0.155 | 0.572 | 0.384 | 0.000 |
| 0.1821 | 16.014 | 7.537 | 9.661 | 0.998 | 0.211 | 0.572 | 0.384 | 0.000 |
| 0.1821 | 16.478 | 7.650 | 9.547 | 0.987 | 0.552 | 0.567 | 0.389 | 0.000 |
| 0.1820 | 16.819 | 7.731 | 9.466 | 0.740 | 0.866 | 0.459 | 0.497 | 0.000 |
| 0.1820 | 17.028 | 7.753 | 9.430 | 0.086 | 1.291 | 0.087 | 0.869 | 0.000 |
| 0.1819 | 17.448 | 7.765 | 9.391 | 0.028 | 1.847 | 0.000 | 0.956 | 0.000 |
| 0.1818 | 17.894 | 7.785 | 9.357 | 0.026 | 2.306 | 0.000 | 0.956 | 0.000 |
| 0.1813 | 18.449 | 7.831 | 9.317 | 0.025 | 2.815 | 0.000 | 0.956 | 0.000 |
| 0.1803 | 18.956 | 7.923 | 9.277 | 0.024 | 3.237 | 0.000 | 0.956 | 0.000 |
| 0.1792 | 19.270 | 7.977 | 9.250 | 0.023 | 3.501 | 0.000 | 0.859 | 0.097 |
| 0.1790 | 19.304 | 7.983 | 9.247 | 0.022 | 3.543 | 0.000 | 0.710 | 0.246 |
| 0.1789 | 19.325 | 7.988 | 9.245 | 0.022 | 3.572 | 0.000 | 0.588 | 0.368 |
| 0.1788 | 19.345 | 7.991 | 9.244 | 0.022 | 3.602 | 0.000 | 0.467 | 0.489 |
| 0.1787 | 19.365 | 7.994 | 9.242 | 0.022 | 3.629 | 0.000 | 0.366 | 0.590 |
| 0.1786 | 19.389 | 7.996 | 9.240 | 0.022 | 3.660 | 0.000 | 0.271 | 0.685 |
| 0.1784 | 19.430 | 8.001 | 9.237 | 0.022 | 3.706 | 0.000 | 0.166 | 0.790 |
| 0.1768 | 19.654 | 8.032 | 9.220 | 0.021 | 3.909 | 0.000 | 0.020 | 0.936 |
| 0.1721 | 20.050 | 8.095 | 9.186 | 0.019 | 4.228 | 0.000 | 0.002 | 0.954 |
| 0.1585 | 20.596 | 8.204 | 9.131 | 0.021 | 4.637 | 0.000 | 0.000 | 0.956 |
| 0.1453 | 20.889 | 8.267 | 9.093 | 0.030 | 4.837 | 0.000 | 0.000 | 0.917 |
| 0.1283 | 21.147 | 8.389 | 9.051 | 0.045 | 5.000 | 0.000 | 0.000 | 0.917 |
| 0.1112 | 21.347 | 8.482 | 9.009 | 0.061 | 5.126 | 0.000 | 0.000 | 0.917 |

D

Table 5. (contd.)

| $M_r/M$ | $\log P$ | $\log T$ | $\log r$ | $L_r/L$ | $\log \varrho$ | $X$ | $Y$ | $X_C$ |
|---|---|---|---|---|---|---|---|---|
| 0.0935 | 21.517 | 8.509 | 8.966 | 0.077 | 5.235 | 0.000 | 0.000 | 0.916 |
| 0.0754 | 21.668 | 8.560 | 8.918 | 0.089 | 5.333 | 0.000 | 0.000 | 0.915 |
| 0.0547 | 21.823 | *8.615* | 8.853 | 0.097 | 5.432 | 0.000 | 0.000 | 0.914 |
| 0.0381 | 21.941 | *8.656* | 8.787 | 0.103 | 5.508 | 0.000 | 0.000 | 0.914 |
| 0.0241 | 22.042 | *8.691* | 8.708 | 0.108 | 5.572 | 0.000 | 0.000 | 0.914 |
| 0.0092 | 22.160 | *8.731* | 8.554 | 0.106 | 5.649 | 0.000 | 0.000 | 0.914 |
| 0.0061 | 22.191 | *8.742* | 8.489 | 0.097 | 5.668 | 0.000 | 0.000 | 0.914 |
| 0.0029 | 22.229 | *8.755* | 8.371 | 0.073 | 5.693 | 0.000 | 0.000 | 0.914 |
| 0.0021 | 22.240 | *8.758* | 8.321 | 0.061 | 5.700 | 0.000 | 0.000 | 0.914 |
| 0.0000 | 22.281 | *8.772* | 1.000 | 0.000 | 5.727 | 0.000 | 0.000 | 0.914 |

In describing the results thus far, the emphasis was mainly placed upon the evolution with time of the central region, i.e. upon approximately the innermost 16% of the stellar mass. What course does the evolution of the outer shell sources take? It had been indicated in paper IV of this series that hydrogen-burning might possibly begin again at the interface of hydrogen and helium. This is now indeed the case, as can be seen from Table 6. It is evident from Table 5 that the hydrogen-burning shell is extremely thin. The newly initiated hydrogen-burning is linked to the exhaustion of the helium-burning shell source underneath. Thus, the hydrogen burning takes over the production of the considerable portion of energy which reaches the surface (cf. Fig.5). This change in energy production coincides with the reversing point M in the HR-diagram and is possibly responsible for this reversal.

## 4. Computations

The physical properties of the thermal runaway (the instability) are discussed in the appendix to this paper. In addition to that, several events of the flash can be understood directly from the equations for the construction of models:

We shall make the (strongly simplifying) assumption that within the flash there are in essence two phases, namely, a phase of central density which is constant with time while the central temperature increases and a phase of central temperature which is constant with time while the central density decreases (cf. Fig.3). The time scales for both phases may then be estimated roughly.

Moreover it can be made plausible with the help of the virial theorem why during the flash event, during which the energy, which is released in the interior, heats the center, other mass shells of the star must be cooled adiabatically at the same time (cf. Fig. 6).

Table 6. Characteristic values in the maximum of the hydrogen and helium-shell source and the inner boundary of the outer convective zone (W K Z) for several selected models.

| | 1 | | | | 2 | | | | 3 |
|---|---|---|---|---|---|---|---|---|---|
| Nr. | Maximum von $\varepsilon_{He}$ | | | | Maximum von $\varepsilon_H$ | | | | Innere Grenze der WKZ |
| | $M_r/M$ | $\log T$ | $\log \varrho$ | $\varepsilon_{He}$ | $M_r/M$ | $\log T$ | $\log \varrho$ | $\varepsilon_H$ | $M_r/M$ |
| 402 | 0.1771 | 8.328 | 3.079 | $8.2 \cdot 10^6$ | 0.1815 | 7.132 | −1.152 | $7.4 \cdot 10^{-3}$ | 0.1816 |
| 408 | 0.1785 | 8.320 | 3.107 | $6.8 \cdot 10^6$ | 0.1815 | 7.388 | −0.283 | $6.8 \cdot 10^1$ | 0.1818 |
| 419 | 0.1788 | 8.316 | 3.145 | $5.7 \cdot 10^6$ | 0.1815 | 7.528 | 0.201 | $3.5 \cdot 10^4$ | 0.1820 |
| 439 | 0.1789 | 8.310 | 3.164 | $5.2 \cdot 10^6$ | 0.1815 | 7.574 | 0.354 | $2.4 \cdot 10^5$ | 0.1820 |
| 461 | 0.1790 | 8.302 | 3.143 | $4.2 \cdot 10^6$ | 0.1815 | 7.589 | 0.409 | $4.4 \cdot 10^5$ | 0.1821 |
| 480 | 0.1790 | 8.284 | 3.133 | $1.8 \cdot 10^6$ | 0.1815 | 7.594 | 0.434 | $5.5 \cdot 10^5$ | 0.1821 |
| 490 | 0.1790 | 8.260 | 3.101 | $5.1 \cdot 10^5$ | 0.1815 | 7.589 | 0.432 | $4.7 \cdot 10^5$ | 0.1821 |
| 494 | 0.1790 | 8.217 | 3.067 | $4.8 \cdot 10^4$ | 0.1815 | 7.595 | 0.470 | $6.5 \cdot 10^5$ | 0.1822 |
| 500 | 0.1790 | 8.158 | 3.184 | $2.7 \cdot 10^3$ | 0.1815 | 7.715 | 0.907 | $7.0 \cdot 10^7$ | 0.1825 |
| 510 | 0.1790 | 8.051 | 3.412 | $3.8 \cdot 10^0$ | 0.1816 | 7.746 | 0.997 | $1.3 \cdot 10^8$ | 0.1822 |
| 520 | 0.1790 | 8.031 | 3.450 | $8.6 \cdot 10^{-1}$ | 0.1816 | 7.751 | 1.067 | $1.5 \cdot 10^8$ | 0.1822 |
| 530 | 0.1790 | 8.015 | 3.483 | $2.4 \cdot 10^{-1}$ | 0.1817 | 7.754 | 1.099 | $1.6 \cdot 10^8$ | 0.1823 |
| 550 | 0.1790 | 7.995 | 3.519 | $5.2 \cdot 10^{-2}$ | 0.1818 | 7.755 | 1.101 | $1.7 \cdot 10^8$ | 0.1824 |
| 570 | 0.1790 | 7.985 | 3.548 | $2.2 \cdot 10^{-2}$ | 0.1820 | 7.756 | 1.130 | $1.6 \cdot 10^8$ | 0.1825 |

1 Maximum of $\varepsilon_{He}$; 2 Maximum of $\varepsilon_H$; 3 Inner Boundary of WKZ

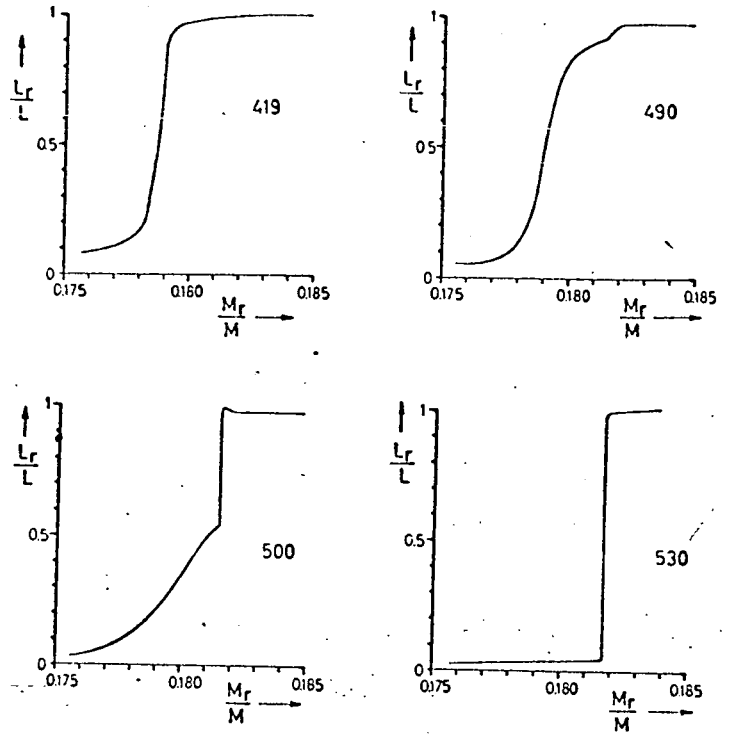


Figure 5. The luminosity $L_r/L$ in the region of the shell sources as function of $M_r/M$ for several models (the numbers given indicate the model numbers). The figure shows the takeover of the energy production by the newly formed hydrogen shell source (approximately at $M_r/M = 0.182$).

The course of the speed of the temperature increase (i.e. the change of $\partial \ln T/\partial t$) and that of the subsequent decrease in density result from the application of the law of conservation of energy to the entire convective core. Since the luminosity which comes from the convective core is so small that it can be neglected when compared with the $L_r$-values in the proximity of the core, the following approximation may be written:

$$\int_0^{M_K} \varepsilon_C \, dM_r = -\int_0^{M_K} \varepsilon_g \, dM_r , \tag{1}$$

i.e., all nuclear energy released is converted to inner energy or to work of expansion. It is

$$\varepsilon_g = -c_p \dot{T} + \frac{\delta}{\varrho} \dot{P} = -c_v T \left( \frac{\dot{T}}{T} - \frac{V_{ad}}{\alpha} \frac{c_p}{c_v} \frac{\dot{\varrho}}{\varrho} \right), \quad \alpha = \left( \frac{\partial \ln \varrho}{\partial \ln p} \right)_T . \tag{2}$$

Since in the convective core in good approximation (namely as long as $V_{ad}$ is constant with regard to space and time) the term in parentheses in (2) is not dependent upon the location, it follows

$$\int_0^{M_K} \varepsilon_C \, dM_r = \left( \frac{\dot{T}}{T} - \frac{V_{ad}}{\alpha} \frac{c_p}{c_v} \frac{\dot{\varrho}}{\varrho} \right) \int_0^{M_K} c_v T \, dM_r . \tag{3}$$

In the first phase of the flash it is in a first approxination $\rho_c/\rho_c = 0$ (cf. Fig.3). From (3) it follows then

$$\frac{\dot{T}_c}{T_c} = -\frac{\int_0^{M_K} \varepsilon_c \, dM_r}{\int_0^{M_K} c_v T \, dM_r} . \qquad (4)$$

We are now going to compare models 408 and 480 in Table 2; between the two models lies an evolutionary phase for which the change with time of $\rho_c$ may be neglected. Equation (4) will then be valid approximately. The numerator of the right-hand side of (4) is, in good approximation, proportional to $(\varepsilon_C)_c$ (= central value of $\varepsilon_c$), since only the region near the center makes a contribution. If we set in a rough approximation for the denominator $\frac{1}{2} \cdot c_v T_c \cdot M_K$, then it follows

$$\frac{\dot{T}_c}{T_c} \sim \frac{(\varepsilon_c)_c}{T_c M_K} , \qquad (5)$$

wherefrom we can understand quantitatively why the time constant $(T_c/\dot{T}_c)$ decreases from Model 408 to Model 480 by a factor of 200. If $M_K$ between the two models did not increase by a factor of 10, the decrease of the time constant would be larger by 1 power of 10.

If the expansion is noticable in the models which follow Nr. 480, we may set approximately with Model 502 in an approximation $T_c/T_c = 0$ and obtain

$$\frac{\dot{\varrho}_c}{\varrho_c} = -\frac{\alpha}{V_{ad}} \frac{c_v}{c_p} \frac{\int_0^{M_K} \varepsilon_c \, dM_r}{\int_0^{M_K} c_v T \, dM_r}, \tag{6}$$

from which we obtain the characteristic time for the expansion of the central region. Since in the phase under consideration $M_K$ remains constant, it follows for the border-line case of the ideal gas, which is approximated by the central region:

$$\frac{\dot{\varrho}_c}{\varrho_c} \sim -\frac{(\varepsilon_c)_c}{T_c}. \tag{7}$$

The time scale for the expansion remains therefore constant in a first approximation; it indeed increases to some extent since $T_c$ decreases slightly (cf. Fig.3).

The processes in the layers above the convective core are more easily understood if one applies the law of conservation of energy and the virial theorem to the entire star. If $E_n$ represents the entire nuclear energy supply, U the total inner energy, and $E_G$ the gravitational energy, then the law of conservation of energy applies

$$L = -(\dot{E}_n + \dot{E}_G + \dot{U}). \tag{8}$$

Since for the ideal gas and for the (nonrelativistic) Fermi-Dirac gas the same relation between pressure and energy u per gram applies, namely

$$u = \frac{3}{2}\frac{P}{\varrho}, \tag{9}$$

we can write for the entire star the virial theorem in the conventional form

$$2\dot{U} = -\dot{E}_G . \tag{10}$$

Now we obtain $\dot{E}_n = \dot{E}_C + \dot{E}_S$ (contributions $E_C$ from the central carbon-burning and $\dot{E}_S$ from the shell-source burning). During the flash the following applies: $-\dot{E}_C >> L + \dot{E}_S$. Equation (8) may now be replaced in a first approximation by

$$\dot{E}_{nC} + \dot{E}_G + \dot{U} = 0 . \tag{11}$$

From(10) and (11) we then obtain

$$\dot{U} = \dot{E}_{nC} \qquad (<0), \tag{12}$$

$$\dot{E}_G = -2\dot{E}_{nC} \qquad (>0). \tag{13}$$

It follows from (12) that $\dot{U}$ is negative.

Since during the increase to the flash the inner energy of the central region increases, the inner energy in the layers above must decrease. Since there is no degeneracy, the temperature has to decrease (cf. Fig,6). Since the time scale of these changes is short by comparison with the Kelvin-Helmholtz time scale of the participating shells, cooling takes place by way of adiabatic expansion. Equation 13 shows that the total of gravitational energy of the star increases. Since the central region does not participate in the expansion (due to degeneracy) the gravitational energy will be increased by rapid expansion of the outer regions.

This becomes clearer, if one bears in mind the fact that at the onset of the flash the entire amount of released nuclear energy is converted to inner energy $U_K$ of the central region, since the central region does not expand and practically not contribute luminosity to the layers above. Thus, the following is valid:

$$\dot{U}_K + \dot{E}_{nC} = 0 . \qquad (14)$$

It be, $U_\Lambda = U - U_K$, the inner energy of the outer layers. It then follows from 12, and 13

$$\dot{U}_A = -\dot{E}_G = 2\,\dot{E}_{nc}.$$

Thus, in the outer layers, the amount $2\,\dot{E}_{nc}$ of inner energy is converted to gravitational energy of these shells.

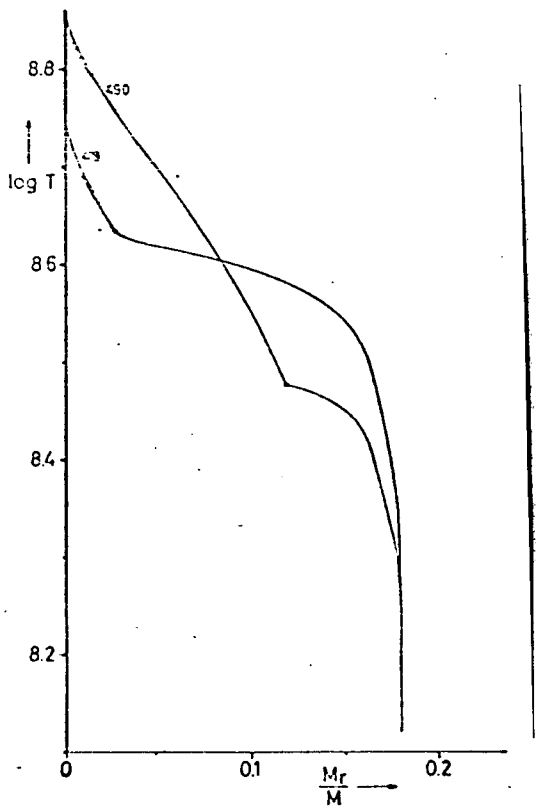


Figure 6. The temperature as function of $M_r/M$ in the central region for two selected models (Nr. 419 and Nr. 490). The dots within the curves indicate the boundary of the convective core.

In the subsequent phase, during which expansion of the central region occurs, $\dot{U}_K$ will become equal to zero and later even negative. This indicates that $\dot{U}_A$ will become equal to or smaller than $\dot{E}_{nC}$.

## Appendix: The Stability of the Interior of the Star during Strong Temperature Dependence of $\epsilon$ [1]

For a better understanding of the flash event the stability behavior of a simplified model shall be investigated. For this purpose, we assume a sphere separated from the center. The mass of this sphere be $M_K$ ($M_K$ is now longer necessarily the mass of the convective core). A small disturbance in the form of energy supply will be brought about in the sphere. How does $\epsilon$ react to that? Will the nuclear energy production be reduced by the supply of disturbing energy and

---

1) The physical reason of the flash-event had already been found in 1952 by Mestal. The simplified model described in the following, shall only present a relatively easy access to the flash theory. Simultaneously, it will show the relationship between the flash-teory and the Cowling criterion for secular stability.

$\epsilon$

the star will compensate the disturbing energy (stability) or does the disturbing energy cause an additional overproduction (instability)? We shall first assume that all energy of the disturbance is converted to inner energy and external work and that the radiative portion of disturbing energy is negligible. The same shall also apply to the overproduction of nuclear energy which is caused by the disturbance. The luminosity $L_K$ of the sphere shall thus at all times remain unchanged and equal to the undisturbed value. This assumption is realized the better the faster th disturbing energy is applied to the sphere and the larger the temperature dependence of $\varepsilon$ is, for the faster can the nuclear energy source, by changing its production with time, compensate or increase the disturbing energy.

On the other hand, the course of the events shall not be so fast that the inertia terms play a role. The time scale of the events shall thus, on the one hand, be short by comparison with the Kelvin-Helmholtz time scale, on the other hand, long as compared with the pulsation period of the model.

The law of conservation of energy for this sphere will thus read:

$$L_K = \int_0^{M_K} \left( \varepsilon - c_p \dot{T} + \frac{\delta}{\varrho} \dot{P} \right) dM_r , \qquad (1)$$

whereby $L_K$ is the value of $L_r$ at the surface of the sphere.

The terms $\epsilon$, T, $\rho$, P, $L_r$ we now write in the form:

$$\varepsilon = \varepsilon_0 + \varepsilon_1, \quad T = T_0 + T_1, \ldots, \tag{2}$$

whereby the terms with the index 0 are the value of the unperturbed model, the index 1 describes the disturbance. The sphere under consideration be small enough that the terms $\epsilon$, T, $\rho$, P, $\dot{P}$, $\dot{T}$ vary only very little in it. In the following we thus employ always the mean values over the sphere. The assumption made initially, that the luminosity at the surface of the sphere does not vary is identical with the postulate $(L_{r1})_K = 0$.

The following applies to the unperturbed terms:

$$(L_{r0})_K = \left(\varepsilon_0 - c_{p0} \dot{T}_0 + \frac{\delta_0}{\varrho_0} \dot{P}_0\right) M_K \tag{3}$$

and for the disturbances, according to our conditions - except for the terms of higher order:

$$\varepsilon_1 = c_{p0} \dot{T}_1 - \frac{\delta_0}{\varrho_0} \dot{P}_1 . \tag{4}$$

Between the change $r_1$ of the radius r of the sphere and the density, the following relationship is valid:

$$\frac{\varrho_1}{\varrho_0} = -3 \frac{r_1}{r_0} . \tag{5}$$

The relationship between the change in pressure at the surface of the sphere and the change in radius is not determined by the events in the interior of the sphere. It is determined by the behavior of the outer shells. The pressure at the surface of the sphere is at every moment determined by an integral over the outer mass:

$$P_K = \int_{M_K}^{M} \frac{G M_r}{4\pi r^4} dM_r , \tag{6}$$

in which $M_K$ is again the mass in the sphere. We set:

$$\frac{P_1}{P_0} = -\frac{4}{f}\frac{r_1}{r_0} , \tag{7}$$

in which f is a free factor which is determined by the behavior of the outer mass. For homologous changes of the outer mass one obtains f = 1. The equation of state describes the relationship between the changes of density, pressure, and temperature:

$$\frac{\varrho_1}{\varrho_0} = \varkappa_0 \frac{P_1}{P_0} - \delta_0 \frac{T_1}{T_0} , \tag{8}$$

in which the terms

$$\varkappa = \left(\frac{\partial \ln \varrho}{\partial \ln P}\right)_T , \quad \delta = -\left(\frac{\partial \ln \varrho}{\partial \ln T}\right)_P \tag{9}$$

of the equation of state are determined.

From (5), (7), (8) we obtain:

$$\frac{P_1}{P_0} = \frac{4\delta_0}{4\varkappa_0 - 3f}\frac{T_1}{T_0}. \tag{10}$$

Since our disturbance shall be fast by comparison, for instance, with changes in dependence of time of $P_0$, $T_0$ due to the evolution of the star (even if these are determined by the Kelvin-Helmholtz time scale), it follows:

$$\frac{\partial}{\partial t}\left(\frac{P_1}{P_0}\right) = \frac{\dot{P}_1}{P_0} - \frac{P_1}{P_0}\frac{\dot{P}_0}{P_0} \approx \frac{\dot{P}_1}{P_0} \tag{11}$$

and if one differentiates the right-hand side of (10) with time and utilizes the same arguments, one then obtains:

$$\frac{\dot{P}_1}{P_0} = \frac{4\delta_0}{4\varkappa_0 - 3f}\frac{\dot{T}_1}{T_0} \tag{12}$$

and the law of conservation of energy (4) reads as follows:

$$\varepsilon_1 = c_{p0}T_0\left(1 - \frac{\delta_0 P_0}{c_{p0}\varrho_0 T_0}\frac{4\delta_0}{4\varkappa_0 - 3f}\right)\frac{\dot{T}_1}{T_0} \tag{13}$$

and since

$$\nabla_{ad} = \frac{\delta P}{c_p \varrho T} \tag{14}$$

the following results

$$\varepsilon_1 = c_{p0}T_0\left(1 - \nabla_{ad\,0}\frac{4\delta_0}{4\varkappa_0 - 3f}\right)\frac{\dot{T}_1}{T_0}. \tag{15}$$

If one assumes

$$\varepsilon = \varepsilon^* T^\nu \tag{16}$$

for reasons of simplicity the ρ-dependence of ε be neglected) one obtains

$$\varepsilon_0 = \varepsilon^* T_0^\nu , \quad \frac{\varepsilon_1}{\varepsilon_0} = \nu \frac{T_1}{T_0} \tag{17}$$

and the law of conservation of energy is therefore represented by the differential equation:

$$\frac{d}{dt}\left(\frac{T_1}{T_0}\right) = A \frac{T_1}{T_0} \tag{18}$$

with

$$A = \frac{\nu \varepsilon_0}{c_{p0} T_0 \left(1 - \nabla_{ad0} \frac{4\delta_0}{4\alpha_0 - 3\beta}\right)} \tag{19}$$

with the solution

$$\frac{T_1}{T_0} = \text{konst.} \cdot e^{At} . \tag{20}$$

Negative A indicates stability (each disturbance fades out); positive A indicates that the minor addition of energy results in an exponential increase of temperature and energy production, i.e. instability.

For an ideal gas with $\nu$, $\varepsilon_o$ both $> 0$ and with $f = 1$ the term in parentheses in (19) has the value -0.6. A is negative, the burning is thus stable. The insignificant increase in central temperature disappears again. This is the situation for nuclear burning in non-degenerate matter.

With increasing relativistic or non-relativistic degeneracy the term

$$\delta = -\frac{\partial \ln \varrho}{\partial \ln T} \to 0$$

and thus the statement in parentheses in the equation for A approaches +1. A thus becomes positive. Nuclear burning in degenerate matter is instable. A small change in temperature increases exponentially. This is the flash.

In equation (19) for the critical term A the parameter f occurs. From that it follows that the exact condition for the occurrence of a flash is not only dependent upon the variables of the state in the center but also from the properties of the shells above.

With the same arguments one can, by the way, demonstrate that the situation is reversed in the case of neutrino-losses. If we assume that in the center of the star the burning of a certain

element is exhausted and that the loss, for instance, by photo-neutrinos ($\epsilon = \epsilon^* T^8$, $\epsilon^* \leq 0$) be described by $\epsilon$ in (17), then the same considerations do apply. However, because of $\epsilon_o < 0$ for ideal gases we obtain $A > 0$ (thus instability, neutrino-collaps). For the degenerate gas, however, we have a situation which is stable in the sense of our consideration ($A < 0$).

If one drops the assumption of the constancy of the luminosity $L_K$ at the surface of the sphere, one must, however, also consider and linearize the transport equation. One then obtains for A the equation:

$$A = \frac{\nu \epsilon_0 - \frac{L_{K_0}}{M_K}(-\varphi - \varkappa_{P0}\varphi + 4 - \varkappa_{T0})}{c_{p0} T_0 (1 - \varphi V_{ad0})}$$

$$\left(\varkappa_P = \left(\frac{\partial \ln \varkappa}{\partial \ln P}\right)_T, \quad \varkappa_T = \left(\frac{\partial \ln \varkappa}{\partial \ln T}\right)_P\right)$$

(with $\Psi = \frac{4\delta_o}{4\alpha_o - 3f}$), which changes to our earlier one as long as $\nu$ is sufficiently large. For an ideal gas and $f = 1$ the stability condition $A < 0$ is identical with the condition of secular stability for homologous changes as earlier derived by Cowling (1934).

## Literature

Cowling, T.G.: Monthly Notices Roy. Astron. Soc. 94, 768 (1934).

Hofmeister, E., R. Kippenhahn and A. Weigert: Z. Astrophys. 59, 215 (1964). - Diss. Munich 1966, (to be published in Z. Astrophys.)

Kippenhahn, R., H.-C. Thomas and A. Weigert: Z. Astrophys. 61, 241 (1965).

Mestel, L.: Monthly Notices Roy. Astron. Soc. 112, 598 (1952).

Reeves, H.: Stellar Energy Sources, in: Stars and Stellar Systems, Vol. VIII. Chicago, London: University of Chicago Press 1965.

Salpeter, E.E.: Australian J. Phys. 7, 373 (1954).

Schwarzschild, M., and R. Härm: Astrophys. J. 136, 158 (1962).

Prof. R. Kippenhahn, Dr. A. Weigert,
University Observatory Göttingen, Geismarlandstr.11
Dipl.-Phys. H.-C. Thomas,
Max-Planck-Institut für Physik und Astrophysik,
Munich 23, Föhringer Ring 6